



SRTTU

Journal of Computational and Applied Research  
in Mechanical Engineering

jcarme.sru.ac.ir

JCARME

ISSN: 2228-7922

**Research paper**

# Analysis of chemical reaction and thermophoresis on MHD flow near the accelerated vertical plate in a rotating system with variable temperature

U. S. Rajput\* and Mohammad Shareef

Department of Mathematics and Astronomy, University of Lucknow, Lucknow-226007, India

**Article info:**

**Article history:**

Received: 05/09/2017  
Revised: 23/01/2020  
Accepted: 26/01/2020  
Online: 28/01/2020

**Keywords:**

Thermophoresis,  
Rotation,  
MHD,  
Porous medium,  
Chemical Reaction.

\*Corresponding author:  
[rajputshareeflu@gmail.com](mailto:rajputshareeflu@gmail.com)

**Abstract**

This study analyses the combined effect of chemical reaction and Soret number on MHD flow of a viscous and incompressible fluid near the exponentially accelerated infinite vertical plate in a rotating system. The fluid under consideration is electrically conducting and the medium is porous. A set of dimensionless governing equations of the model is obtained. As the equations are linear, an exact solution is derived by using Laplace technique. The effects of flow parameters on the concentration, temperature and velocity are discussed through graphs. It is noticed that the components of the velocity in both the directions can be increased by increasing the Soret number; and the velocities can be reduced by increasing the chemical reaction parameter. Tables depict the numerical values of the rate of change of momentum, concentration and temperature. Applications of the study are considered in the fields like solar plasma and planetary fluid dynamics systems, rotating MHD generators, etc.

**1. Introduction**

The fluid flow problems related to free convection and heat/mass transfer under the impact of a uniform/non-uniform magnetic field has great implementation in many areas of engineering and science. Moreover, flow through a porous medium has plentiful geophysical uses, for example, in chemical engineering for purification and filtration process; oil and water through the oil reservoirs; petroleum technology to understand the movement of natural gases; and agriculture

engineering to analyze the underground water resources. By virtue of these big applications, a number of scholars have examined MHD convective flow with heat/mass transfer in a porous medium; a few of them are Kim [1], Sattar [2], Raptis and Kafousias [3], Soundalgekar [4], Prasad et al. [5], Ganesan, and Loganathan [6], Raptis [7], Muthucumaraswamy et.al [8] and Hossain and Takhar [9]. Also, in various practicable diffusive processes, the molecular diffusion of species is taken place under the influence of chemical reaction. All the industrial chemical processes are modelled in

such a manner that the economical raw materials can be transformed to high value products by a chemical reaction. An investigation of the transport of species and their interaction with chemical reactions are rather complex and is immediately associated to the underlying fluid dynamics. Therefore, some authors have analyzed the influence of chemical reaction on MHD convective flow. For instance, Kandasamy et al. [10] studied the effect of chemical reaction on MHD flow along a vertical stretching surface with thermal stratification and heat source. The effect of magnetic field on unsteady convective flow with heat/mass transfer past an impulsively started semi-infinite vertical flat surface under the influence of a homogeneous first order chemical reaction was presented by Al-Azab and Al-Odat [11]. Also, the rotating fluids have their abundant geophysical and astrophysical applications. Some natural phenomena such as tornadoes, geophysical systems, ocean circulations, hurricanes etc. imply rotating flows with heat/mass transfer. Several articles and books on heat transfer and hydrodynamic characteristics of rotating flows have been published (Greenspan [12], Shalini and Shweta [13], Soong and Ma [14], Owen and Rogers [15], Muthucumaraswamy et al. [16], Soong [17]). Further, for the flow problem with heat/mass transfer, the concentration flux is generated by temperature gradient [18] and this phenomenon is known as the Soret effect. The Soret effect can be neglected for the problems in which the concentration level of the diffusing species is very low, but this effect should be considered as most of the heat and mass transport processes are controlled by the simultaneous influence of buoyancy force due to mass and thermal diffusion. These transport processes are detected in combustion systems, nuclear reactor safety, furnace design, glass production, etc. Postelnicu [19] has examined the effect of magnetic field on flow with heat/mass transfer by convection from vertical flat surface in a porous medium considering Dufour and Soret effects. Further, Postelnicu [20] has analyzed the consequences of chemical reaction on heat/mass transfer by free convection from a vertical flat surface in a porous medium taking Dufour and Soret effects. Also, the Dufour and Soret effects on MHD

mixed convection flow past a vertical flat surface embedded in a porous medium was presented by Makinde [21]. An analytic solution of the model considering heat/mass transfer over a porous stretching surface affected by internal heating, Soret-Dufour effect, chemical reaction and Hall current was found by Abdallaha [22]. Recently, Prakash et al. [23] examined the Dufour and Soret effects on MHD boundary layer flow over a vertical porous surface embedded in a porous medium, considering chemical reaction of first order and thermal radiation. They used the perturbation technique to solve the non-linear coupled PDEs. Further, Soret and Dufour effects on MHD flow over a non linear stretching sheet with chemical reaction were presented by Shalini and Rakesh [24]. They use Runge–Kutta Fehlberg method to solve the governing equations and noticed that the temperature of the system can decrease by increasing Soret parameter and a rise in chemical reaction parameter can decrease the concentration of the system.

Influenced by the above literature, this article presents the effect of Soret number, rotation and chemical reaction of first order on MHD flow near the exponentially accelerated infinite vertical plate in a rotating system. The governing PDEs of the model have been solved analytically by using the Laplace Transform technique. The effects of various flow parameters involved in the problem on velocity, concentration and temperature are discussed graphically.

## 2. Mathematical formulation and solution of the model

Consider a free convective flow of an electrically conducting, incompressible and viscous fluid past an accelerated infinite vertical plate embedded in a porous medium. Here  $x$ -axis is chosen along the plate in the vertical upward direction,  $z$ -axis is perpendicular to the plane of the plate and  $y$ -axis normal to  $x$ - $z$  plane. Let both the plate and the fluid rotate as a rigid body with a constant angular velocity  $\bar{\Omega} = (0, 0, \Omega)$  about  $z$ -axis; and a uniform magnetic field of magnitude  $B_0$  is applied along the perpendicular to the plane of the plate. Initially, at a time  $t \leq 0$ , the

fluid and the plate are supposed to be at rest; concentration and temperature are  $C_\infty$  and  $T_\infty$  respectively. For the time  $t > 0$ , let the plate start to move with a velocity  $u = u_0 \exp(-\lambda t)$  in its own plane and the concentration of the plate is raised to  $C_p$ . Also, at the same time, the temperature of the plate is raised to  $T_\infty + (T_p - T_\infty)t/t_o$  where  $T_p > T_\infty$ . Thermal diffusion (Soret effect) and a homogeneous binary first-order chemical reaction with a constant rate  $K_o$  between the fluid and the diffusing species are considered. Let the Magnetic Reynolds number of the fluid be very low, so the magnetic field induced by the fluid motion is negligible as compared to the applied one. Since considering the surface is infinite occupying the plane  $z=0$ , all the physical variables are considered to be the functions of  $z$  and  $t$ . Thus, the magnetic field and fluid velocity are given as  $\vec{B} = (0, 0, B_o)$  and  $\vec{q} = (u, v, 0)$  respectively and the equation of continuity identically becomes zero. Also, no external electric field is used and the effects of polarization of fluid is neglected. Let the porous medium be present everywhere and homogeneous. The rest of the properties of the porous medium and the fluid are supposed to be constant except for density variations in the buoyancy force term (Boussinesq's approximation). So, under the above assumptions, the governing equations are as follows:

$$\frac{\partial u}{\partial t} - 2\Omega v = \nu \frac{\partial^2 u}{\partial z^2} + g\beta(T - T_\infty) + g\beta^*(C - C_\infty) - \frac{\sigma B_o^2}{\rho} u - \frac{\nu}{K} u \tag{1}$$

$$\frac{\partial v}{\partial t} + 2\Omega u = \nu \frac{\partial^2 v}{\partial z^2} - \frac{\sigma B_o^2}{\rho} v - \frac{\nu}{K} v, \tag{2}$$

$$\frac{\partial C}{\partial t} = D \frac{\partial^2 C}{\partial z^2} + \frac{D_T k_T}{T_m} \frac{\partial^2 T}{\partial z^2} - K_o(C - C_\infty), \tag{3}$$

$$\frac{\partial T}{\partial t} = \alpha \frac{\partial^2 T}{\partial z^2}. \tag{4}$$

The boundary conditions taken are as under:

$$\left. \begin{aligned} t \leq 0 : u(z, t) = 0, v(z, t) = 0, C(z, t) = C_\infty, \\ T(z, t) = T_\infty \text{ and for } t > 0 : u(0, t) = u_0 e^{-\lambda t}, \\ v(0, t) = 0, C(0, t) = C_p, \\ T(0, t) = T_\infty + (T_p - T_\infty)t/t_o \\ u(\infty, t) \rightarrow 0, v(\infty, t) \rightarrow 0, C(\infty, t) \\ \rightarrow C_\infty, T(\infty, t) \rightarrow T_\infty, \end{aligned} \right\} \tag{5}$$

where  $t_o = \nu/u_o^2$  and  $\lambda \geq 0$ .

To obtain the equations in a non-dimensional form, the following non-dimensional parameters are used:

$$\left. \begin{aligned} \bar{u} = \frac{u}{u_o}, \bar{v} = \frac{v}{u_o}, \bar{t} = \frac{u_o^2}{\nu} t, \bar{K} = \frac{u_o^2}{\nu^2} K, \\ \bar{z} = \frac{u_o}{\nu} z, \theta = \frac{(T - T_\infty)}{(T_p - T_\infty)}, S_c = \frac{\nu}{D}, \\ P_r = \frac{\nu}{\alpha}, \bar{\Omega} = \frac{\nu}{u_o^2} \Omega, \bar{\lambda} = \frac{\nu}{u_o^2} \lambda, \nu = \frac{\mu}{\rho} \\ \phi = \frac{(C - C_\infty)}{(C_p - C_\infty)}, G_m = \frac{g\beta^* \nu (C_p - C_\infty)}{u_o^3}, \\ H_a^2 = \frac{\sigma B_o^2 \nu}{\rho u_o^2}, G_r = \frac{g\beta \nu (T_p - T_\infty)}{u_o^3}. \end{aligned} \right\} \tag{6}$$

The Eqs. (1-5) become:

$$\frac{\partial \bar{u}}{\partial \bar{t}} - 2\bar{\Omega} \bar{v} = \frac{\partial^2 \bar{u}}{\partial \bar{z}^2} - (H_a^2 + \frac{1}{\bar{K}}) \bar{u} + G_m \phi + G_r \theta, \tag{7}$$

$$\frac{\partial \bar{v}}{\partial \bar{t}} + 2\bar{\Omega} \bar{u} = \frac{\partial^2 \bar{v}}{\partial \bar{z}^2} - (H_a^2 + \frac{1}{\bar{K}}) \bar{v}, \tag{8}$$

$$\frac{\partial \phi}{\partial \bar{t}} = \frac{1}{S_c} \frac{\partial^2 \phi}{\partial \bar{z}^2} + S_r \frac{\partial^2 \theta}{\partial \bar{z}^2} - c_r \phi, \tag{9}$$

$$\frac{\partial \theta}{\partial \bar{t}} = \frac{1}{P_r} \frac{\partial^2 \theta}{\partial \bar{z}^2}. \tag{10}$$

$$\left. \begin{aligned} \bar{t} \leq 0 : \bar{u} = 0, \bar{v} = 0, \phi = 0, \theta = 0 \forall \bar{z} \text{ and} \\ \text{for } \bar{t} > 0 : \bar{u} = e^{-\bar{\lambda} \bar{t}}, \bar{v} = 0, \phi = 1, \theta = \bar{t} \\ \text{at } \bar{z} = 0 \text{ and } \bar{u} \rightarrow 0, \bar{v} \rightarrow 0, \phi \rightarrow 0, \theta \rightarrow 0 \\ \text{as } \bar{z} \rightarrow \infty. \end{aligned} \right\} \tag{11}$$

After dropping the bars ( $\bar{\quad}$ ), Eqs. 7 to 11 can be written as,

$$\frac{\partial u}{\partial t} - 2\Omega v = \frac{\partial^2 u}{\partial z^2} - (H_a^2 + \frac{1}{K})u + G_m \phi + G_r \theta, \tag{12}$$

$$\frac{\partial v}{\partial t} + 2\Omega u = \frac{\partial^2 v}{\partial z^2} - \left(H_a^2 + \frac{1}{K}\right)u, \tag{13}$$

$$\frac{\partial \phi}{\partial t} = \frac{1}{S_c} \frac{\partial^2 \phi}{\partial z^2} + S_r \frac{\partial^2 \theta}{\partial z^2} - c_r \phi, \tag{14}$$

$$\frac{\partial \theta}{\partial t} = \frac{1}{P_r} \frac{\partial^2 \theta}{\partial z^2}, \tag{15}$$

$$\left. \begin{aligned} t \leq 0 : u(z, t) = 0, v(z, t) = 0, \phi(z, t) = 0, \\ \theta(z, t) = 0 \text{ and for } t > 0 : u(0, t) = e^{-\lambda t}, \\ v(0, t) = 0, \phi(0, t) = 1, \theta(0, t) = t \text{ and} \\ u(z, t) \rightarrow 0, v(z, t) \rightarrow 0, \phi(z, t) \rightarrow 0, \\ \theta(z, t) \rightarrow 0 \text{ as } z \rightarrow \infty. \end{aligned} \right\} \tag{16}$$

To solve the above system, consider  $V = u + iv$  where  $i = \sqrt{-1}$ . Then after combining Eqs. (12 and 13), we get,

$$\frac{\partial V}{\partial t} = \frac{\partial^2 V}{\partial z^2} - bV + G_m \phi + G_r \theta, \tag{17}$$

The boundary conditions (16) are reduced to:

$$\left. \begin{aligned} t \leq 0 : V(z, t) = 0, \phi(z, t) = 0, \\ \theta(z, t) = 0 \text{ and for } t > 0 : V(0, t) = e^{-\lambda t}, \\ \phi(0, t) = 1, \theta(0, t) = t \text{ and } V(z, t) \rightarrow 0, \\ \phi(z, t) \rightarrow 0, \theta(z, t) \rightarrow 0 \text{ as } z \rightarrow \infty. \end{aligned} \right\} \tag{18}$$

The governing non-dimensional Eqs. (14, 15 and 17) subjects to the above boundary conditions given in Eq. (18) are solved using the Laplace Transform technique. The solution for velocity ( $P_r \neq 1$  and  $S_c \neq 1$ ), concentration and temperature is as under:

$$\begin{aligned} V(z, t) = & (N_1 - N_2 t) \left\{ \begin{aligned} & 2\text{Cosh}(a_1 z) + e^{-a_1 z} \text{Erf}(a_1 \sqrt{t} - \eta) \\ & - e^{a_1 z} \text{Erf}(a_1 \sqrt{t} + \eta) \end{aligned} \right\} \\ & + N_3 e^{-B_2 t} \left\{ \begin{aligned} & 2\text{Cosh}(a_2 z) - e^{-a_2 z} \text{Erf}(\eta - a_2 \sqrt{t}) \\ & - e^{a_2 z} \text{Erf}(\eta + a_2 \sqrt{t}) \end{aligned} \right\} \\ & + N_4 z \left\{ \begin{aligned} & -2\text{Sinh}(a_1 z) + e^{-a_1 z} \text{Erf}(a_1 \sqrt{t} - \eta) \\ & + e^{a_1 z} \text{Erf}(a_1 \sqrt{t} + \eta) \end{aligned} \right\} \end{aligned}$$

$$\begin{aligned} & + N_5 e^{-\lambda t} \left\{ \begin{aligned} & 2\text{Cosh}(a_3 z) - e^{-a_3 z} \text{Erf}(\eta - a_3 \sqrt{t}) \\ & - e^{a_3 z} \text{Erf}(\eta + a_3 \sqrt{t}) \end{aligned} \right\} \\ & + N_6 e^{-A t} \left\{ \begin{aligned} & 2\text{Cosh}(a_4 z) + e^{-a_4 z} \text{Erf}(a_4 \sqrt{t} - \eta) \\ & - e^{a_4 z} \text{Erf}(a_4 \sqrt{t} + \eta) \end{aligned} \right\} \\ & + N_7 e^{-B_2 t} \left\{ \begin{aligned} & 2\text{Cosh}(a_5 z) - e^{-a_5 z} \text{Erf}(\eta - a_5 \sqrt{t}) \\ & - e^{a_5 z} \text{Erf}(\eta + a_5 \sqrt{t}) \end{aligned} \right\} \\ & + N_8 e^{-A t} \left\{ \begin{aligned} & 2\text{Cosh}(a_6 z) + e^{-a_6 z} \text{Erf}(ia_7 \sqrt{t} - a_8 \eta) \\ & - e^{a_6 z} \text{Erf}(ia_7 \sqrt{t} + a_8 \eta) \end{aligned} \right\} \\ & - N_9 z \sqrt{t} e^{-\eta^2 P_r} + (N_{10} + N_{11} z^2 + N_{12} t) \text{Erfc}(a_8 \eta) \\ & + N_{13} e^{-B_2 t} \left\{ \begin{aligned} & 2\text{Cosh}(a_9 z) + e^{-a_9 z} \text{Erf}(a_{10} \sqrt{t} - a_8 \eta) \\ & - e^{a_9 z} \text{Erf}(a_{10} \sqrt{t} + a_8 \eta) \end{aligned} \right\} \\ & - N_{14} e^{-A t} \left\{ \begin{aligned} & 2\text{Cosh}(a_{11} z) + e^{-a_{11} z} \text{Erf}(a_{12} \sqrt{t} - a_{13} \eta) \\ & - e^{a_{11} z} \text{Erf}(a_{12} \sqrt{t} + a_{13} \eta) \end{aligned} \right\} \\ & + N_{15} \left\{ \begin{aligned} & 2\text{Cosh}(a_{14} z) + e^{-a_{14} z} \text{Erf}(a_{15} \sqrt{t} - a_{13} \eta) \\ & - e^{a_{14} z} \text{Erf}(a_{15} \sqrt{t} + a_{13} \eta) \end{aligned} \right\} \\ & + N_{16} e^{-B_2 t} \left\{ \begin{aligned} & 2\text{Cosh}(a_{16} z) + e^{-a_{16} z} \text{Erf}(a_{17} \sqrt{t} - a_{13} \eta) \\ & - e^{a_{16} z} \text{Erf}(a_{17} \sqrt{t} + a_{13} \eta) \end{aligned} \right\} \end{aligned} \tag{19}$$

$$\begin{aligned} \theta(z, t) = & t \text{Erfc}(a_8 \eta) \\ & + \frac{1}{2} (a_8 z)^2 \text{Erfc}(a_8 \eta) - \frac{2}{\sqrt{\pi}} a_8 \eta t e^{(a_8 \eta)^2} \end{aligned} \tag{20}$$

$$\begin{aligned} \phi(z, t) = & + \frac{a}{A} \text{Erfc}(a_8 \eta) \\ & - \frac{a}{2A} e^{-A t} \left\{ \begin{aligned} & 2\text{Cosh}(a_6 z) + e^{-a_6 z} \text{Erf}(ia_7 \sqrt{t} - a_8 \eta) \\ & - e^{a_6 z} \text{Erf}(ia_7 \sqrt{t} + a_8 \eta) \end{aligned} \right\} \\ & + \left( \frac{A - a}{2A} \right) \left\{ \begin{aligned} & 2\text{Cosh}(a_{14} z) \\ & + e^{-a_{14} z} \text{Erf}(a_{15} \sqrt{t} - a_{13} \eta) \\ & - e^{a_{14} z} \text{Erf}(a_{15} \sqrt{t} + a_{13} \eta) \end{aligned} \right\} \\ & + \frac{a}{2A} e^{-A t} \left\{ \begin{aligned} & 2\text{Cosh}(a_{11} z) \\ & + e^{-a_{11} z} \text{Erf}(a_{12} \sqrt{t} - a_{13} \eta) \\ & - e^{a_{11} z} \text{Erf}(a_{12} \sqrt{t} + a_{13} \eta) \end{aligned} \right\} \end{aligned} \tag{21}$$

**3. Rate of change of momentum, concentration and temperature**

The shear stress components in the primary and secondary directions are  $\tau_x(z, t)$  and  $\tau_y(z, t)$  respectively and obtained by

$$\tau_x = -\mu \frac{\partial u}{\partial z} \quad \text{and} \quad \tau_y = -\mu \frac{\partial v}{\partial z}.$$

By taking non-dimensional parameters given in (6), the dimensionless stresses are

$$\tau_1(\bar{z}, \bar{t}) = \frac{\tau_x}{\tau_o} = -\frac{\partial \bar{u}}{\partial \bar{z}} \quad \text{and} \quad \tau_2(\bar{z}, \bar{t}) = \frac{\tau_y}{\tau_o} = -\frac{\partial \bar{v}}{\partial \bar{z}}$$

where  $\tau_o = \rho u_o^2$ .

Now for finding the solution for  $\tau_1$  and  $\tau_2$ , consider the complex notation i.e.  $\tau(\bar{z}, \bar{t}) = \tau_1(\bar{z}, \bar{t}) + i\tau_2(\bar{z}, \bar{t})$ , where  $i = \sqrt{-1}$ , and after removing the bars ( $\bar{\phantom{x}}$ ), the dimensionless shear stress can be written as:

$$\tau(z, t) = \tau_1(z, t) + i\tau_2(z, t) = -\frac{\partial V(z, t)}{\partial z}$$

Hence, the non-dimensional skin friction coefficient is given as

$$\begin{aligned} S_f(t) = \tau(0, t) = & (N_1 - tN_2) \left\{ \frac{2e^{-a_1^2 t}}{\sqrt{\pi t}} + 2a_1 \text{Erf}(a_1 \sqrt{t}) \right\} \\ & + N_3 e^{-B_1 t} \left\{ \frac{2e^{-a_2^2 t}}{\sqrt{\pi t}} + 2a_2 \text{Erf}(a_2 \sqrt{t}) \right\} \\ & - 2N_4 \text{Erf}(a_1 \sqrt{t}) + N_5 e^{-\lambda t} \left\{ \frac{2e^{-a_3^2 t}}{\sqrt{\pi t}} + 2a_3 \text{Erf}(a_3 \sqrt{t}) \right\} \\ & + N_6 e^{-At} \left\{ \frac{2e^{-a_4^2 t}}{\sqrt{\pi t}} + 2a_4 \text{Erf}(a_4 \sqrt{t}) \right\} \\ & + N_7 e^{-B_2 t} \left\{ \frac{2e^{-a_5^2 t}}{\sqrt{\pi t}} + 2a_5 \text{Erf}(a_5 \sqrt{t}) \right\} \\ & + N_8 e^{-At} \left\{ \frac{2a_8 e^{a_7^2 t}}{\sqrt{\pi t}} + 2ia_6 \text{Erf}(ia_7 \sqrt{t}) \right\} + \frac{a_8(N_{10} + N_{12}t)}{\sqrt{\pi t}} \end{aligned}$$

$$\begin{aligned} & + N_9 \sqrt{t} + N_{13} e^{-B_1 t} \left\{ \frac{2a_8 e^{-a_{10}^2 t}}{\sqrt{\pi t}} + 2a_9 \text{Erf}(a_{10} \sqrt{t}) \right\} \\ & - N_{14} e^{-At} \left\{ \frac{2a_{13} e^{-a_{12}^2 t}}{\sqrt{\pi t}} + 2a_{11} \text{Erf}(a_{12} \sqrt{t}) \right\} \\ & + N_{15} \left\{ \frac{2a_{13} e^{-a_{15}^2 t}}{\sqrt{\pi t}} + 2a_{14} \text{Erf}(a_{15} \sqrt{t}) \right\} \\ & + N_{16} e^{-B_2 t} \left\{ \frac{2a_{13} e^{-(B_2+c_r)t}}{\sqrt{\pi t}} + 2a_{16} \text{Erf}(a_{16} \sqrt{(-B_2+c_r)t}) \right\} \end{aligned}$$

The dimensionless skin friction coefficients in the primary and secondary direction respectively are obtained as:

$$S_{f_x} = \text{Re}(S_f) \quad \text{and} \quad S_{f_y} = \text{Im}(S_f)$$

Again, by using the dimensionless variables given in (6), we find the expression for non-dimensional Nusselt and Sherwood number as follows:

$$\text{Nusselt number} = Nu = -\left( \frac{\partial \theta}{\partial z} \right)_{z=0} = 2\sqrt{\frac{tP_r}{\pi}} \quad \text{and}$$

$$\begin{aligned} \text{Sherwood number} = Sh = & -\left( \frac{\partial \phi}{\partial z} \right)_{z=0} \\ & = \frac{a\sqrt{P_r}}{A\sqrt{\pi t}} - \frac{a\sqrt{-AP_r}}{A} e^{-At} \\ & + \frac{a}{A} e^{-At} \left\{ -\frac{e^{At}\sqrt{P_r}}{\sqrt{\pi t}} + \sqrt{-AP_r} \text{erfc}(\sqrt{-At}) \right\} \\ & + \frac{a}{A} e^{-At} \sqrt{(-A+c_r)S_c} \\ & + \left(1 - \frac{a}{A}\right) \left\{ \sqrt{c_r S_c} + \frac{e^{-c_r t} \sqrt{S_c}}{\sqrt{\pi t}} - \sqrt{c_r S_c} \text{erfc}(\sqrt{c_r t}) \right\} \\ & + \frac{a}{A} e^{-At} \frac{e^{-t(-A+c_r)} \sqrt{S_c}}{\sqrt{\pi t}} \\ & - \frac{a}{A} e^{-At} \sqrt{(-A+c_r)S_c} \text{erfc}\left(\sqrt{t(-A+c_r)}\right) \end{aligned}$$

**5. Results and discussion**

Figs.1-16 depict the effects of various physical parameters on velocity, concentration and temperature distribution near the plate for a particular instant of time. From Figs. 1 to 10 it is

noticed that the magnitude of the velocity components, along the direction of motion of the plate (primary velocity  $u$ ), and along the transverse direction (secondary velocity  $v$ ), a different maximum value near the plate ( $z < 1$ ) is attained and then decreases with increasing 'z' upto the free stream value. Figs. 1 to 4 show the influence of the chemical reaction parameter at a different instant of time and exponential parameter; and it is noticed that a rise in the chemical reaction parameter corresponds to a decrease in both the components of the velocity. Initially the maximum value of the primary component of the velocity occurs at the plate, but as the time increases, it is achieved in the interval  $0 < z < 0.6$  (Figs. 1 and 2). The influence of Soret number at different instants of time and rotation is shown in Figs. 5 to 8 and; it is noticed that an increase in the Soret number corresponds to rise in both components of the velocity. Also, the secondary velocity increases rapidly and the primary velocity decreases with the increase in rotation (Figs. 7 and 8). It is also observed from Figs. 5 and 6 that, as the time passes, both components of the velocity accelerate rapidly. The effect of rotation parameter at different values of magnetic field parameter is given in Figs. 9 and 10; and it can be observed that the primary velocity decreases and the secondary velocity increases with an increase in the rotation parameter. Figs. 13 to 16 display the concentration profile near the plate at different times and chemical reaction parameter. Variation in the concentration with Soret number is shown in Figs. 13 and 14; and it is noticed that the concentration in the system increases with the increase in the Soret number.

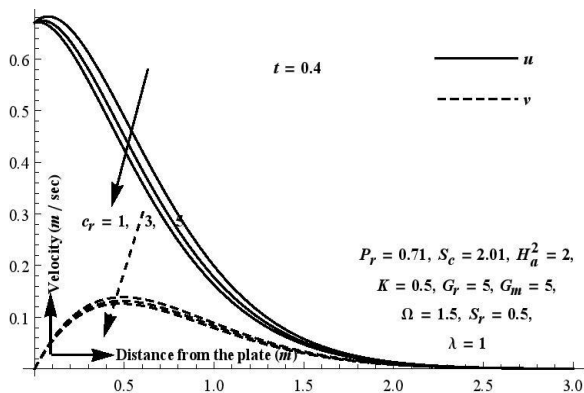


Fig. 1. Velocity profile for  $c_r$  at  $t = 0.4$ .

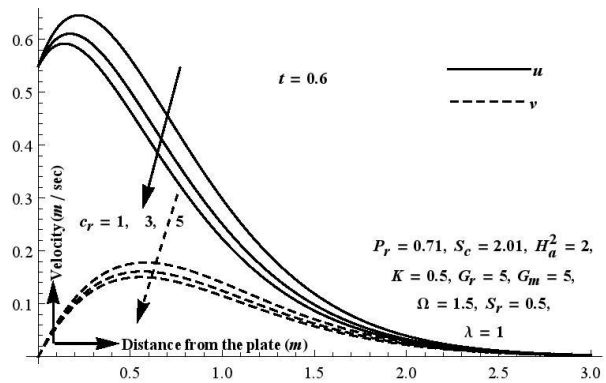


Fig. 2. Velocity profile for  $c_r$  at  $t = 0.6$ .

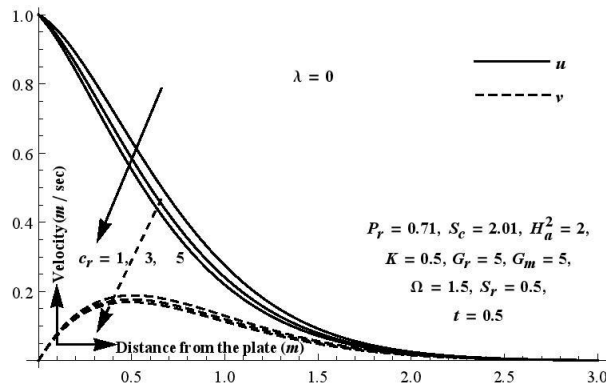


Fig. 3. Velocity profile for  $c_r$  at  $\lambda = 0$ .

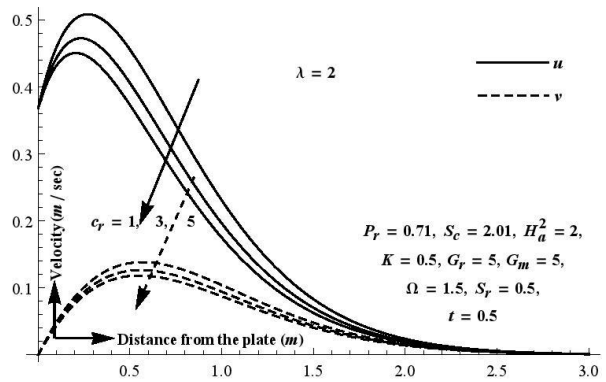


Fig. 4. Velocity profile for  $c_r$  at  $\lambda = 2$ .

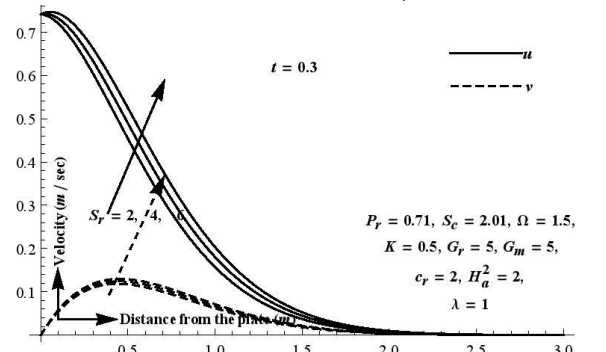


Fig. 5. Velocity profile for  $S_r$  at  $t = 0.3$ .

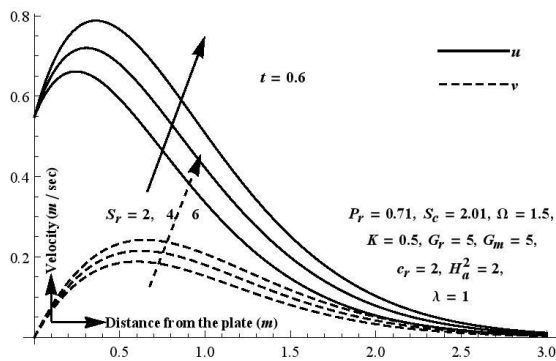


Fig. 6. Velocity profile for  $S_r$  at  $t = 0.6$ .

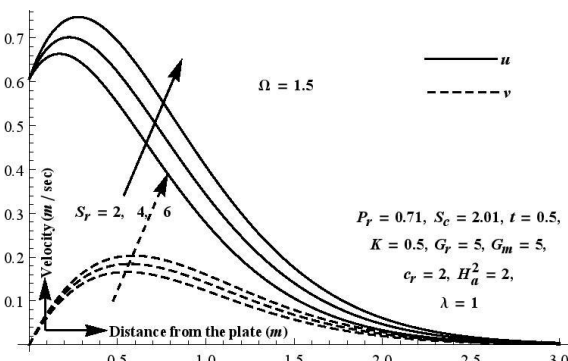


Fig. 7. Velocity profile for  $S_r$  at  $\Omega = 1.5$ .

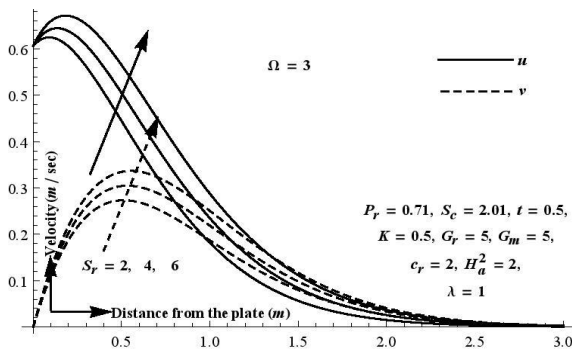


Fig. 8. Velocity profile for  $S_r$  at  $\Omega = 3$ .

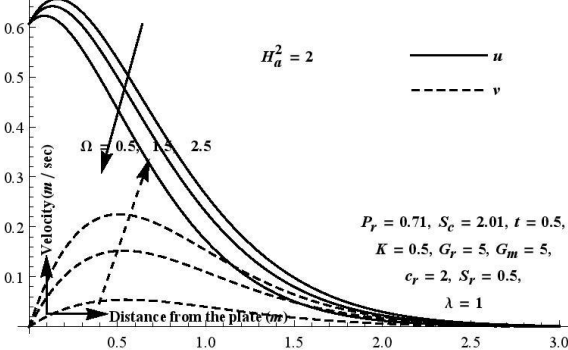


Fig. 9. Velocity profile for  $\Omega$  at  $H_a^2 = 2$ .

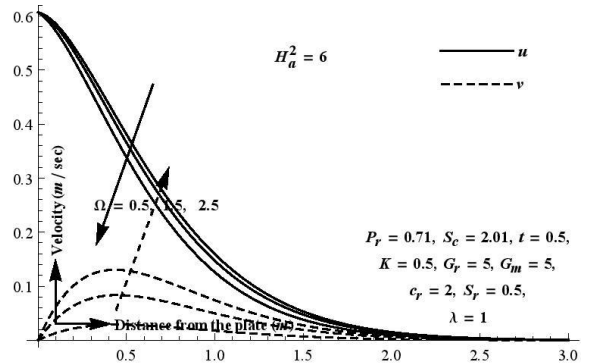


Fig. 10. Velocity profile for  $\Omega$  at  $H_a^2 = 6$ .

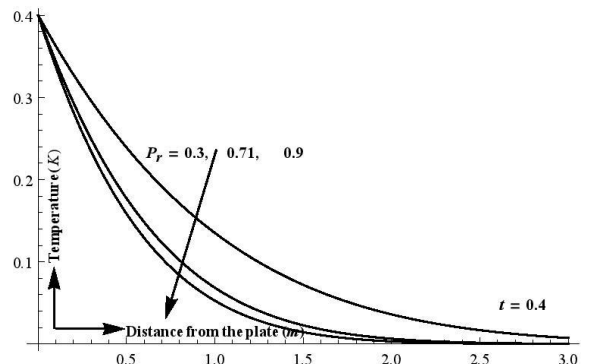


Fig. 11. Temperature profile for  $P_r$  at  $t = 0.4$ .

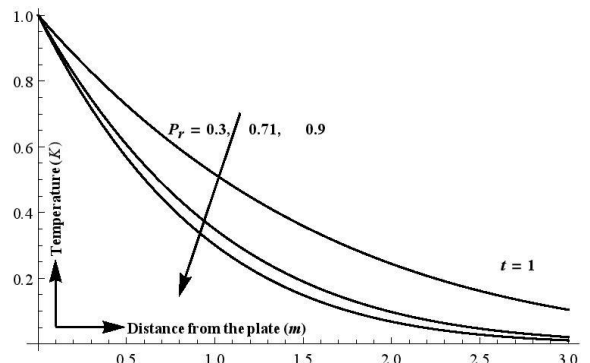


Fig. 12. Temperature profile for  $P_r$  at  $t = 1$ .

Figs. 15 and 16 depict the influence of chemical reaction parameter on concentration in the system at different instants of time. It is noticed that an increase in the chemical reaction parameter corresponds to a reduction in the concentration of the system. Also, it is noticed that as the time passes, the concentration increases. Variation in the temperature with Prandtl number is shown in Figs. 11 and 12; and it reveals that the temperature in the system reduces with an increase in Prandtl number. Also, the solution for velocity (Eq. (19)) is

reasonable only for  $S_c \neq 1$  and  $P_r \neq 1$ . Prandtl number  $P_r$  is the non-dimensional number which is the ratio of momentum diffusivity to the thermal diffusivity of fluid, whereas dimensionless Schmidt number  $S_c$  is defined as the ratio of momentum diffusivity to the mass diffusivity of the fluid. For the case when  $P_r = 1$  and  $S_c = 1$ , the momentum, thermal and concentration boundary layers thicknesses have values of the same order of magnitude. Further, the variation in the Skin-Friction coefficient with various physical parameters are shown in Tables 1 and 2 at time  $t = 0.4$ . It is revealed from Table 2 that, at a particular rotation, the Skin-Friction components along the primary and secondary direction decrease with and increase in the Soret number. Also, when the chemical reaction parameter increases, both friction components increase (Table 1). It is noticed that an increases in msagnetic field parameter or rotation parameter corresponds to an increase in the friction coefficient along primary direction ( $S_{fx}$ ). Also, the variations in the Sherwood number and Nusselt number are shown numerically in the Tables 3 and 4 respectively. From Table 3, it is noticed that, when the Soret number increases the Sherwood number decreases; and an increase in the Prandtl number corresponds to an increase in the Nusselt number (Table 4).

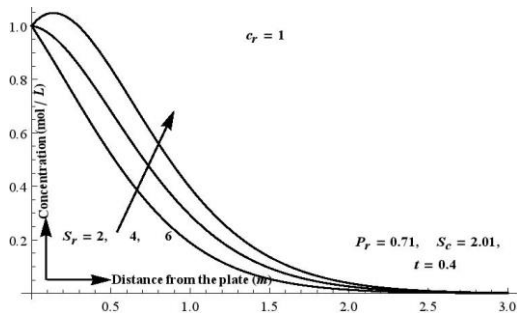


Fig. 13. Concentration profile for  $S_r$  at  $c_r = 1$ .

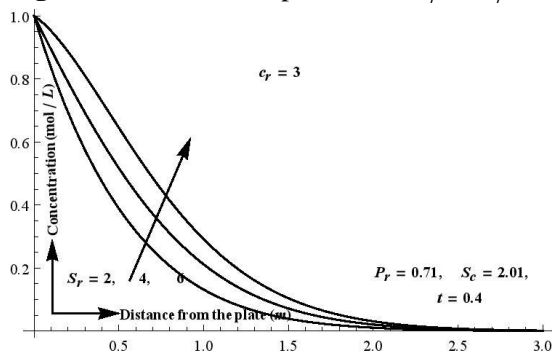


Fig. 14. Concentration profile for  $S_r$  at  $c_r = 3$ .

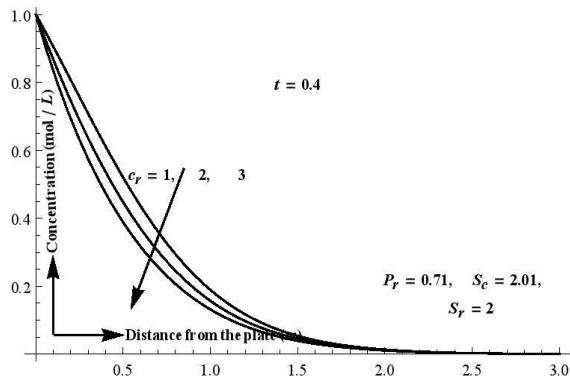


Fig. 15. Concentration profile for  $c_r$  at  $t = 0.4$ .

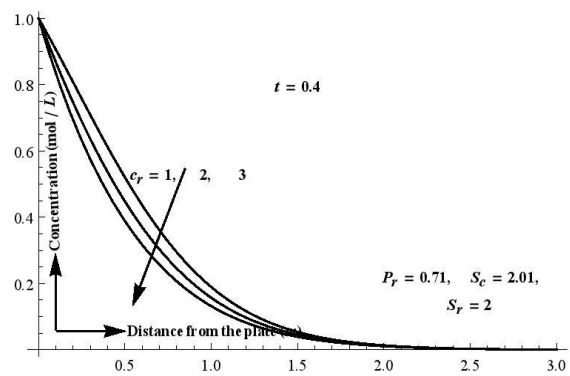


Fig. 16. Concentration profile for  $c_r$  at  $t = 0.8$ .

Table 1. Skin friction for chemical reaction parameter ( $S_r = 2, K = 0.5, \lambda = 1, t = 0.2, \Omega = 0.5, S_c = 2.01, P_r = 0.71, G_r = 5, G_m = 5$ ).

$C_r$	$H_a^2 = 2$		$H_a^2 = 4$	
	$S_{fx}$	$-S_{fy}$	$S_{fx}$	$-S_{fy}$
1	0.4472	0.1982	0.8216	0.1777
3	0.5149	0.1962	0.8855	0.1759
5	0.5725	0.1944	0.9397	0.1743

Table 2. Skin friction for Soret number at different rotation ( $c_r = 1, K = 0.5, \lambda = 1, t = 0.2, H_a^2 = 2, S_c = 2.01, P_r = 0.71, G_r = 5, G_m = 5$ ).

$S_r$	$\Omega = 0.5$		$\Omega = 2.5$	
	$S_{fx}$	$-S_{fy}$	$S_{fx}$	$-S_{fy}$
2	0.4472	0.1982	0.5801	0.9667
4	0.3686	0.2009	0.5036	0.9798
6	0.2901	0.2035	0.4271	0.9929

**Table 3.** Sherwood number for  $S_r$  ( $S_c = 2.01, P_r = 0.71, c_r = 1$ ).

$S_r$	$t = 0.2$	$t = 0.4$
	$Sh$	$Sh$
0	2.1348	1.7394
2	1.5231	0.9073
4	0.9114	0.0752

**Table 4.** Nusselt number.

$P_r$	$t = 0.2$	$t = 0.4$
	$Nu$	$Nu$
0.3	0.2764	0.3909
0.71	0.4252	0.6013
7.0	1.3551	1.8881

**6. Conclusions**

An analytical study has been done for the model under consideration by converting the governing linear partial differential equations into dimensionless form. It is found that at a particular instant of time ( $t = 0.5$ ) the extreme value of the components of the velocity along the primary direction occurs in the interval  $0 \leq z < 0.6$ ; and the maximum for the velocity component along the transverse direction occurs in the interval  $0.3 < z < 0.7$ . The velocity in both directions can increase by increasing the Soret number. On the other hand, the velocity in both directions can be reduced by increasing the chemical reaction parameter. Rotation can retard the primary flow and accelerate the secondary flow.

It is also noticed that the concentration in the system rises with an increase in the Soret number whereas an increase in the chemical reaction parameter can reduce the concentration in the system. An increase in the Prandtl number can reduce the temperature in the system. Also, the concentration and the temperature in the system increase as time passes. The Sherwood number and concentration in the system are more affected by Soret number. Also, the  $S_{f_x}$  increases when  $c_r$  or  $\Omega$  or  $H_a^2$  are increased; on the other

hand increases in  $S_r$  correspond to a decrease in  $S_{f_x}$ . Whereas the skin friction component in the secondary direction, i.e.  $S_{f_y}$  increases when  $c_r$  is increased; and it decreased with an increase in  $S_r$  or  $\Omega$ . Also, the model under consideration can be expanded into the studies of the flow past spheres, cylinders, cones, and wedges etc., according to the required applications.

**References**

[1] J. Youn Kim, "Heat and mass transfer in MHD micropolar flow over a vertical moving porous plate in a porous medium", *T. P. M.*, Vol. 56, No. 1, pp.17-37, (2004).

[2] M. A. Sattar, "Unsteady hydromagnetic free convection flow with Hall current mass transfer and variable suction through a porous medium near an infinite vertical porous plate with constant heat flux", *Int. J. of E. Res.*, Vol. 18, No. 9, pp. 771-775, (1994).

[3] A. Raptis, and N. Kafousias, "Magnetohydrodynamic free convection flow and mass transfer through porous medium bounded by an infinite vertical porous plate with constant heat flux", *Can. J. Phys.*, Vol. 60, No.12, pp.1725-1729, (1982).

[4] V. M. Soundalgekar, "Effects of Mass Transfer and Free-Convection Currents on the Flow Past an Impulsively Started Vertical Plate", *J. Appl. Mech.*, Vol. 46, No. 4, pp. 757-760, (1979).

[5] V. Ramachandra Prasad, N. Bhaskar Reddy, and R. Muthucumaraswamy, "Radiation and mass transfer effects on two-dimensional flow past an impulsively started infinite vertical plate", *Int. J. of T. Sci.*, Vol. 46, No. 12, pp. 1251-1258, (2007).

[6] P. Ganesan, and P. Loganathan, "Radiation and Mass transfer effects on flow of an incompressible viscous fluid past a moving vertical cylinder", *Int. J. of H.M.T.*, Vol. 45, No.21, pp. 4281-4288, (2002).

- [7] A. Raptis, "Radiation and free convection flow through a porous medium", *Int. Comm. In H.M.T.*, Vol. 25, No. 2, pp. 289–295, (1998).
- [8] R. Muthucumaraswamy, P. Ganesan, and V. M. Soundalgekar, "Heat and mass transfer effect on flow past impulsively started vertical plate", *Acta Mec.*, Vol. 146, No. 1-2, pp.1-8, (2001).
- [9] M. A. Hossain, and H. S. Takhar, "Radiation effect on mixed convection along a vertical plate with uniform surface temperature", *H.M.T.*, Vol. 31, No. 4, pp. 243-248, (1996).
- [10] R. Kandasamy, K. Periasamy, and K. K. Sivagnana Prabhu, "Chemical reaction, heat and mass transfer on MHD flow over a vertical stretching surface with heat source and thermal stratification effects", *Int. J. of H. M. T.*, Vol. 48, No. 21-22, pp. 4557-4561, (2005).
- [11] M. Q. Al-Odat, and T.A. Al-Azab, "Influence of chemical reaction on transient MHD free convection over a moving vertical plate", *E. J. for Eng. Res.*, Vol. 12, No. 3, pp. 15-21, (2007).
- [12] H. P. Greenspan, *The T. of R. F.*, Cambridge University Press, London (1968).
- [13] J. Shalini and B. Shweta, "Radiation effects in flow through porous medium over a rotating disks with variable fluid properties", *Adv. in math. Phy.*, Vol. 3, No. 1, pp. 1-12, (2016).
- [14] C. Y. Soong, and H. L. Ma, "Unsteady analysis of non - isothermal flow and heat transfer between rotating co-axial disks", *Int. J. of H.M.T.*, Vol. 38, No. 10, pp. 1865 – 1878, (1995).
- [15] J. M. Owen, and R. H. Rogers, *Flow and heat transfer in rotating disc systems*, Vol. I, Rotor – Stator Systems, John Wiley Sons, New York (1989).
- [16] R. Muthucumaraswamy, N. Dhanasekar, and G. E. Prasad, "Rotation effects on unsteady flow past an accelerated isothermal vertical plate with variable mass transfer in the presence of chemical reaction of first order", *J. A. F. M.*, Vol. 6, No. 4, pp. 485-490, (2013).
- [17] C. Y. Soong, "Thermal buoyancy effects in rotating non - isothermal flows", *Int. J. of R.M.*, Vol. 7, No. 6, pp. 435 - 446, (2001).
- [18] J. K. Platten, "The Soret effect: A review of recent experimental results", *J. of app. mech.*, Vol. 73, No. 1, pp. 5-15, (2006).
- [19] A. Postelnicu, "Influence of a magnetic field on heat and mass transfer by natural convection from vertical surfaces in porous media considering Soret and Dufour effects", *Int. J. of H. M. T.*, Vol. 47, No. 6-7. pp.1467-1472, (2004).
- [20] A. Postelnicu, "Influence of chemical reaction on heat and mass transfer by natural convection from vertical surfaces in porous media considering Soret and Dufour effects", *H. M. T.*, Vol. 43, No. 6, pp. 595-602, (2007).
- [21] O. D. Makinde, "On MHD mixed convection with Soret and Dufour effects past a vertical plate embedded in a porous medium", *L. A. App. Res.*, Vol. 41, No.1, pp. 63-68, (2011).
- [22] A. A. Ibrahim, "Analytic solution of heat and mass transfer over a permeable stretching plate affected by chemical reaction, internal heating, Dufour-Soret and Hall effect", *T. Sci.*, Vol. 13, No.2, pp.183-197, (2009).
- [23] J. Prakash, P. Durga Prasad, R. V. M. S. S. Kiran Kumar, and S. V. K. Varma, "Diffusion-thermo effects on MHD free convective radiative and chemically reactive boundary layer flow through a porous medium over a vertical plate", *J.C.A.R.M.E.*, Vol. 5, No. 2, pp. 111-126, (2015).
- [24] J. Shalini and C. Rakesh "Soret and Dufour effects on thermophoretic MHD flow and heat transfer over a non linear stretching with chemical reaction", *Int. J. Appl. C. M.*, Springer, Vol.4, No.1, Article 50, (2018).

**Appendix**

$$b = H_a^2 + 2i\Omega + \frac{1}{K}, A_1 = \frac{G_r}{1 - P_r}, A_2 = \frac{G_m}{1 - S_c},$$

$$A_3 = \frac{G_m}{1 - P_r}, B_1 = \frac{b}{1 - P_r}, B_2 = \frac{b - c_r S_c}{1 - S_c}, A = \frac{c_r S_c}{S_c - P_r},$$

$$N_1 = \left\{ \begin{array}{l} \frac{A_1}{2B_1^2} + \frac{AA_2 + aA_3 - A_2B_1 - aA_2}{2(A - B_1)(A - B_2)} \\ + \frac{aA_2B_1 - aA_3B_2}{2A(A - B_1)(A - B_2)} \\ + \frac{aA_2A - A_2A^2 - aA_2B_1 + AA_2B_1}{2B_2(A - B_1)(A - B_2)} \\ + \frac{aA_3B_2 - aA_3A}{2B_1(A - B_1)(A - B_2)} \end{array} \right\},$$

$$a = \frac{P_r S_c S_r}{S_c - P_r}, N_2 = \frac{A_1}{2B_1},$$

$$N_3 = \left\{ \frac{-aA_3B_2 + aA_3A}{2B_1(A - B_1)(A - B_2)} - \frac{A_1}{2B_1^2} \right\},$$

$$N_4 = \frac{A_1}{4B_1\sqrt{b}}, N_8 = \frac{aA_3}{2A(A - B_1)},$$

$$N_6 = \frac{aAA_2 - aAA_3 - aB_1A_2 + aB_2A_3}{2A(A - B_1)(A - B_2)},$$

$$N_7 = \frac{B_1B_2A_2 - AB_2A_2 - aAA_2 + A^2A_2 + aB_1A_2 - AB_1A_2}{2B_2(A - B_1)(A - B_2)},$$

$$N_5 = \frac{A^2 - B_1A + B_2B_1 - AB_2}{2(A - B_1)(A - B_2)}, N_9 = \frac{A_1\sqrt{P_r}}{B_1\sqrt{\pi}},$$

$$N_{12} = \frac{A_1}{B_1}, N_{13} = \left\{ -\frac{aA_3}{2B_1(A - B_1)} + \frac{A_1}{2B_1^2} \right\},$$

$$N_{15} = \left\{ \frac{A_2}{2B_2} - \frac{aA_2}{2B_2(A - B_2)} + \frac{aA_2}{2A(A - B_2)} \right\},$$

$$N_{10} = \left\{ \frac{aA_3}{B_1(A - B_1)} - \frac{aA_3}{A(A - B_1)} - \frac{A_1}{B_1^2} \right\}, N_{11} = \frac{A_1P_r}{2B_1},$$

$$N_{12} = \frac{A_1}{B_1}, N_{13} = \left\{ -\frac{aA_3}{2B_1(A - B_1)} + \frac{A_1}{2B_1^2} \right\},$$

$$N_{15} = \left\{ \frac{A_2}{2B_2} - \frac{aA_2}{2B_2(A - B_2)} + \frac{aA_2}{2A(A - B_2)} \right\},$$

$$N_{14} = \frac{aA_2}{2A(A - B_2)}, N_{16} = \left\{ -\frac{A_2}{2B_2} - \frac{aA_2}{2B_2(A - B_2)} \right\},$$

$$a_1 = \sqrt{b}, a_2 = \sqrt{b - B_1}, a_3 = \sqrt{b - \lambda},$$

$$a_4 = \sqrt{b - A}, a_5 = \sqrt{b - B_2}, a_6 = \sqrt{-AP_r},$$

$$a_7 = \sqrt{A}, a_8 = \sqrt{P_r}, a_9 = \sqrt{-B_1P_r}, a_{10} = \sqrt{-B_1},$$

$$a_{11} = \sqrt{(c_r - A)S_c}, a_{12} = \sqrt{(c_r - A)}, a_{13} = \sqrt{S_c},$$

$$a_{14} = \sqrt{c_r S_c}, a_{15} = \sqrt{c_r}, a_{16} = \sqrt{(c_r - B_2)S_c},$$

$$a_{17} = \sqrt{(c_r - B_2)}, \eta = \frac{z}{2\sqrt{t}}.$$

Copyrights ©2021 The author(s). This is an open access article distributed under the terms of the Creative Commons Attribution (CC BY 4.0), which permits unrestricted use, distribution, and reproduction in any medium, as long as the original authors and source are cited. No permission is required from the authors or the publishers.



### How to cite this paper:

U.S. Rajput and Mohammad Shareef, “Analysis of chemical reaction and thermophoresis on MHD flow near the accelerated vertical plate in a rotating system with variable temperature”, *Journal of Computational and Applied Research in Mechanical Engineering*, Vol. 10, No. 2, pp. 449-460, (2021).

**DOI:** 10.22061/jcarme.2020.2883.1301

**URL:** [https://jcarme.sru.ac.ir/?\\_action=showPDF&article=1188](https://jcarme.sru.ac.ir/?_action=showPDF&article=1188)

